The g Factor of Hydrogenic Ions: A Test of Bound State QED

G. Werth[1], H. Häffner[1,2], N. Hermanspahn[1], H.-J. Kluge[2], W. Quint[2], J. Verdú[2]

[1] Johannes Gutenberg Universität, 55099 Mainz, Germany
[2] Gesellschaft für Schwerionenforschung, 64291 Darmstadt, Germany

Abstract. We present a new experimental value for the magnetic moment of the electron bound in hydrogenlike carbon ($^{12}C^{5+}$): $g_{\rm exp} = 2.001\,041\,596\ (5)$. The experiment was carried out on a single $^{12}C^{5+}$ ion stored in a Penning trap. The high accuracy was made possible by spatially separating the induction of spin flips and the analysis of the spin direction. Experiment and theory test the bound-state QED contributions to the g_J factor of a bound electron to a precision of 1%. We discuss also implications of the experiment on the knowledge of the electron mass.

1 Introduction

Quantum-electrodynamics (QED) as the fundamental theory for electromagnetic interaction seems to be well understood. Numerous experiments in atomic physics as well as in high energy physics do not show any significant discrepancy between theoretical predictions and experimental results. The most striking example of agreement between theory and experiment represents the g factor of the free electron. The experimental value of $g = 2.002\ 319\ 304\ 376\ 6\ (87)$ [1] is confirmed by the calculated value of $g = 2.002\ 319\ 304\ 307\ 0\ (280)$ on the 10^{-11}-level, where the fine structure constant as an input in the theoretical calculation was taken from the quantum Hall effect [2]. Up to now uncalculated non-QED contributions play no important role. Indeed today experiment and theory of the free electron yield the most precise fine structure constant.

In contrast to the g factor of the free electron the calculation of the g factor of an electron bound at an atomic nucleus represents a significantly more difficult problem. For the free electron the different orders of Feynman graphs, representing an increasing number of virtual exchange photons, are calculated as a series expansion. The expansion parameter is the fine structure constant α. Since $\alpha \ll 1$, the higher orders in the expansion decrease rapidly and the series converges. In a bound system an additional expansion parameter is $Z\alpha$ which may, at least for high nuclear charges Z, not be a small number. Consequently a non-perturbative approach for calculation of the g factor has to be developed (bound state QED). In a less formal picture the electric field in the vicinity of a nucleus modifies the vacuum field at the position of the electron and leads to a change in the measurable quantities of the electron. Such electric fields can be

extremely strong. For nuclei such as Uranium or Lead the electric field strength for a 1S electron in a Hydrogenic ion is of the order 10^{16} V/cm. This is by many orders of magnitude stronger than fields which can be produced in a laboratory. Experiments under such extreme conditions may represent a stringent test of bound state QED calculations.

Apart from the g factor of a bound electron, the Lamb shift of energy levels for calculable systems such as Hydrogen-like ions as well as Hyperfine splittings for those ions are different tests of bound state QED. Such experiments have been successfully performed in the past [3]. The higher order bound state QED contributions in these systems, however, are overshadowed by nuclear structure contributions which are difficult to account for at the desired level of accuracy. It seems that similar nuclear structure contributions to the g factor in Hydrogen-like ions are less significant [4]. In this case a measurement of the g factor of the electron bound in a Hydrogen-like system would represent a cleaner test of higher order bound state QED corrections.

Precise measurements on g factors of electrons bound in atomic Hydrogen and the Helium ion $^4He^+$ were carried out by Robinson and coworkers. The accuracies of 3×10^{-8} for the Hydrogen atom [5] and of 6×10^{-7} for the Helium ion [6] were sensitive to relativistic effects. Other measurements of the magnetic moment of the electron in Hydrogen-like ions were performed at GSI by Seelig *et al.* for Lead ($^{207}Pb^{81+}$) [7] and by Winter *et al.* for Bismuth ($^{209}Bi^{82+}$) [8] with precisions of about 10^{-3} via lifetime measurements of hyperfine transitions. These measurements were also only sensitive to the relativistic contributions.

We have performed an experiment to measure the g factor of the electron bound to a Carbon nucleus in a Hydrogen-like C^{5+} ion [9]. As shown below, the result of our measurement represents a significant test of bound state QED contributions and also accounts for the recoil correction from the finite mass of the carbon nucleus. The experiments are performed on single C^{5+} ions confined in a Penning ion trap at low temperatures, almost completely isolated from the environment. As outlined in the last paragraph the extension of our experiments to other highly charged systems opens a number of possibilities for future measurements of fundamental quantities such as the electrons mass or the fine structure constant.

2 Summary of Theory

The electron magnetic moment $\boldsymbol{\mu}$ is related to the electron spin $\mathbf{s}$ by

$$\boldsymbol{\mu} = g\frac{e}{2m_e}\mathbf{s}\,, \tag{1}$$

where e and m_e are the electrons charge and mass and g is the gyromagnetic ratio or Landé factor. For the free electron the g factor has been calculated with very high precision [2]. If the electron is bound in the ground state of a Hydrogen-like ion, the g factor is modified by additional binding and radiative corrections which depend on the nuclear charge Z.

The largest correction comes from relativistic effects. The solution of the Dirac equation, first performed by Breit [10] gives

$$g = \frac{2}{3}\left(1 + 2\sqrt{1 - (Z\alpha)^2}\right) . \tag{2}$$

The radiative binding corrections have to be treated nonpertubatively and must include all orders in $Z\alpha$. Blundell *et al.* [11], Persson *et al.* [4] and most recently Beier *et al.* [12,13] have performed such calculations. They include the total QED contribution of order α/π. Fig. 1 represents their results graphically. The

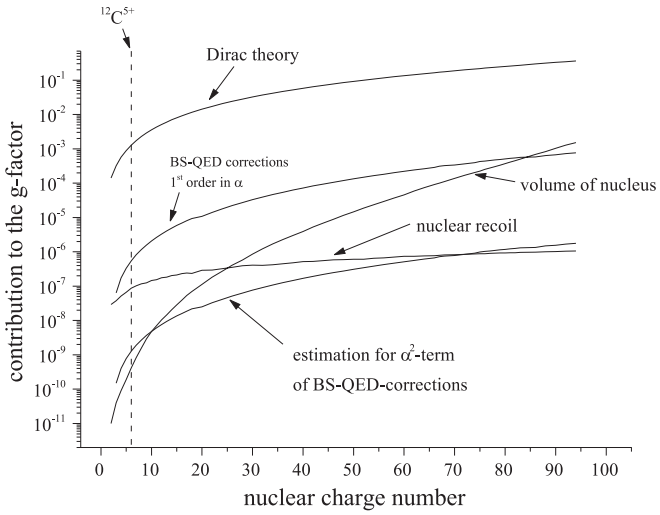

Fig. 1. Relativistic and QED contributions to the electron g factor for values of the nuclear charge number Z. The data is taken from Ref. [12]

calculated bound-state QED terms change the electrons g factor for C^{5+} by almost 1 part in 10^{-6}. For very high values of Z as for Lead or Uranium the change amounts to about 10^{-3}. An estimate of the order $(\alpha/\pi)^2$ gives values which are 2 orders of magnitude smaller. Finally recoil and finite size corrections from the nucleus have to be taken into account. In the case of C^{5+} they amount to 4×10^{-10} and 9×10^{-8}, respectively. For high Z the finite size correction is of the same order as the α/π contributions. Table 1 lists these theoretical contributions to the g factor in C^{5+}.

The present theoretical value for the g factor in $^{12}C^{5+}$ is quoted as [12]

$$g = 2.001\,041\,590\,(71) . \tag{3}$$

Table 1. Theoretical contributions to $g_J(^{12}C^{5+})$, taken from [12]

Dirac theory (incl. binding)	1.998 721 354 2	
Finite-size correction	+0.000 000 000 4	
Recoil	+0.000 000 087 5	(9)
QED, free, up to order $(\alpha/\pi)^4$	+0.002 319 304 4	
QED, bound, order (α/π)	+0.000 000 844 2	(12)
QED, bound, order $(\alpha/\pi)^2$, estimate	±0.000 000 002 0	(50)
Total theoretical value:	2.001 041 590 7	(71)

The largest part of the uncertainty comes from the unknown size of the $(\alpha/\pi)^2$ term. Attempts are under way to calculate this term and thus reduce the theoretical uncertainty substantially [13,14,15].

3 Experiment

The electron g factor as defined by Eq. 1 can be expressed in terms of the cyclotron frequency $\omega_c^e = (e/m_e)B$ of the free electron and the Larmor frequency $\omega_L = g(e/2m_e)B$:

$$g = 2\frac{\omega_c^e}{\omega_L} \; . \tag{4}$$

The determination of the g factor thus requires a measurement of the Larmor and the cyclotron frequency. The electrons cyclotron frequency may conveniently be replaced by $\omega_c^e/\omega_c^i \times \omega_c^i$, where ω_c^i is the ions cyclotron frequency. This is of advantage because the cyclotron frequency of the ion and the Larmor precession frequency can measured at the same particle. The ratio ω_c^e/ω_c^i is the charge to mass ratio of the ion to the electron. For the case of Carbon it has been determined in Penning trap experiments by van Dyck and coworkers [16].

The experiment is performed on a single C^{5+} ion confined in a cylindrical Penning trap with a superimposed magnetic field of 4 T. The trap consists of a stack of 13 ring shaped electrodes of 7 mm inner diameter, mounted on a vacuum flange as shown in Fig. 2. The whole setup is contained in a vacuum vessel which is held at liquid He temperatures. This assures that the residual background pressure is sufficiently low to avoid ion loss by charge capture during a collision with a background molecule. To test for possible losses we stored a cloud of about 30 C^{5+} ions for several weeks. Since we did not observe any ion loss during that time interval we conclude from the known cross sections for electron capture that the base pressure in our system is below 10^{-16} mbar.

By application of proper voltages to the electrodes we create potential minima at any desired point on the axis of the arrangement. This is preferentially done at two positions which we call precision trap and analysis trap (see Fig. 2). Using two of the electrodes (correction electrodes) for fine tuning of the potential shape we can achieve very harmonic potential minima near the center of the traps. Ions are created by electrons hitting a carbon target at a few 100 eV. They can be detected by image currents induced in the trap endcap or ring electrodes.

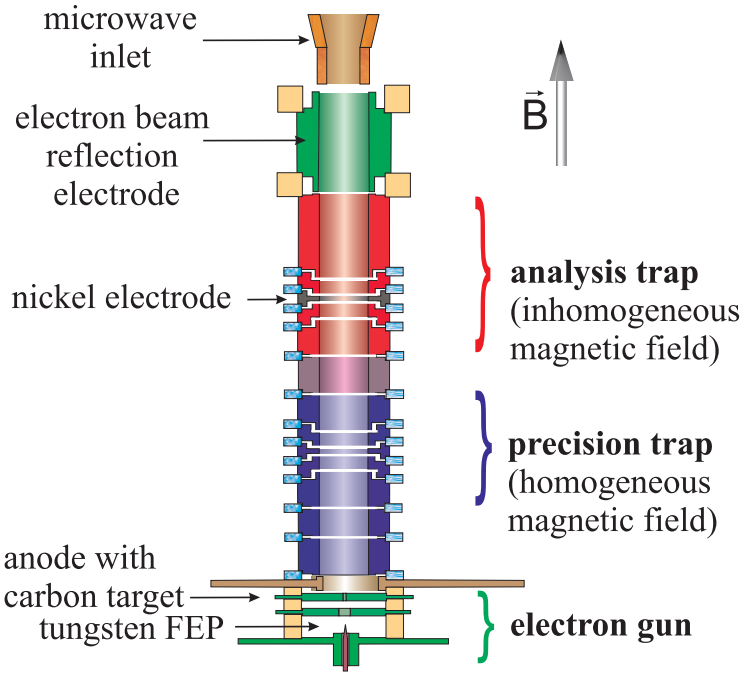

Fig. 2. Sketch of the trap electrodes

For signal enhancement we use superconducting tank circuits attached to the correction electrodes (some are splitted to allow detection of the radial motion). The resonance frequencies of the circuits are tuned to the corresponding ion oscillation frequencies.

After ion creation the trap is usually filled with a large number of carbon ions in all different charge states. Different elements present as impurities in the carbon target may also be ionized and stored. We clean the trap from unwanted species and charge states by strong excitation of their axial frequency which drives them out of the trap. The number of ions in the remaining pure C^{5+} cloud is reduced by exciting the cyclotron motion and lowering the axial potential. The ions get lost due to energy exchange from the cyclotron mode to the axial mode by collisions. At low ion numbers the ions can be individually distinguished by observation of the induced voltage at the cyclotron frequency since our magnetic field is slightly inhomogeneous and ions at different positions in the trap have different cyclotron frequencies. Fig. 3 shows as an example the Fourier transform of the signal from 6 different C^{5+} ions. Finally one single ion is left in the trap and remains there for the entire experiment unless we kick it out intentionally. The remaining ion then is resistively cooled to the ambient temperature. This is achieved by keeping its oscillation frequency in resonance with the frequency of the tank circuit attached to the endcap electrodes. The initially hot ion heats up the tank circuit and the power is dissipated to the Helium bath to which the

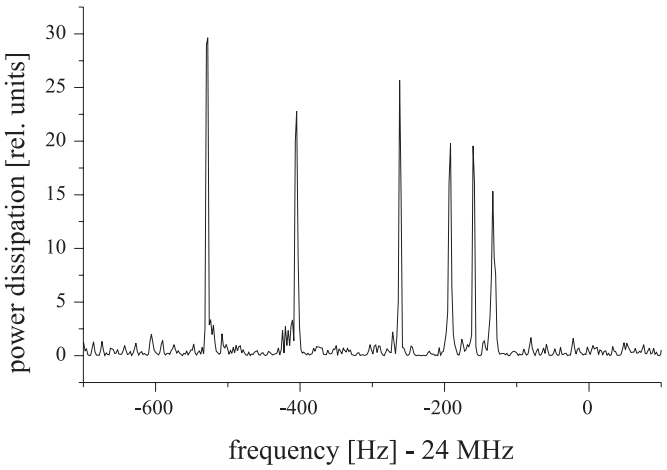

Fig. 3. Fourier transform of the current induced by the cyclotron motion of 6 ions. The magnetic inhomogeneity causes the frequency to decrease with increasing cyclotron energy

circuit is in thermal contact. The cooling time constant is given by

$$\tau^{-1} = \frac{q}{mr_0^2} R \,, \tag{5}$$

where q and m are the ions charge and mass, r_0 is the trap radius and R is the impedance of the tank circuit. For a quality factor $Q = 2500$ of our circuit the cooling time constant for C^{5+} is 100 ms. When the axial amplitude of the ion is in equilibrium with the enviroment it can be detected by a reduction of the noise power in the axial tank circuit. The oscillating ion acts as a series circuit and represents for its resonance frequency a shortcut of the Johnson noise of the external tank circuit [17]. A corresponding signal from a single C^{5+} ion is shown in Fig. 4. The full width of this resonance is 2 Hz. In the example shown its center can be determined to within 100 mHz after 1 min averaging.

In a similar way also the cyclotron motion can be cooled and detected when the tank circuit connecting two segments of the splitted correction electrode is kept in resonance with the ions cyclotron frequency. Fig. 5 shows an example for resistive cooling of the cyclotron motion of a single $^{12}C^{5+}$ ion. For calibration of the magnetic field we use the cyclotron frequency of a single C^{5+} ion. At our magnetic field of 4 T it amounts to about 24 MHz. The free ions cyclotron frequency ω_c, however, is not an eigenfrequency of a particle in the trap. It is related to the traps eigenfrequencies ω_+, the modified cyclotron frequency, ω_z, the axial oscillation frequency, and ω_-, the magneton frequency, by

$$\omega_c^2 = \omega_+^2 + \omega_z^2 + \omega_-^2 \,. \tag{6}$$

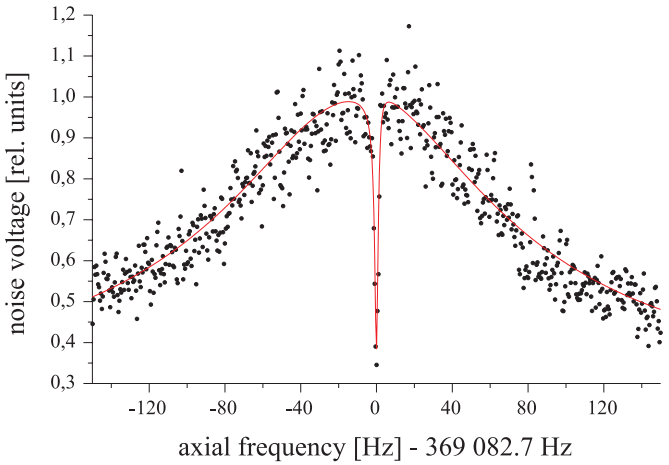

Fig. 4. Axial signal of a single $^{12}C^{5+}$ ion. The width of the signal is 2 Hz

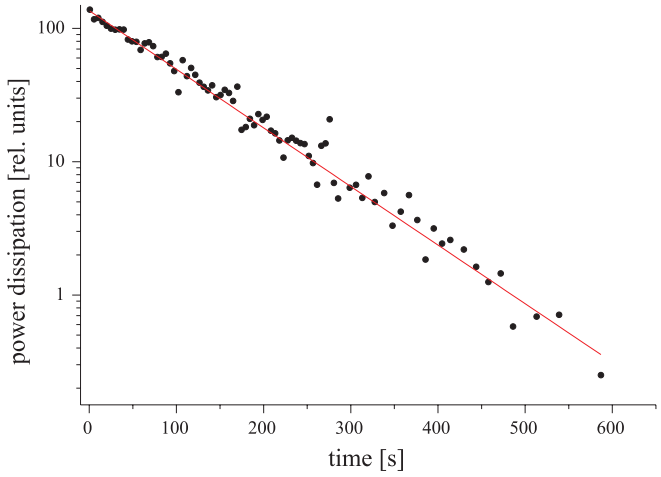

Fig. 5. Resistive cooling of the cyclotron motion of a single $^{12}C^{5+}$ ion. The time constant of the exponential cooling is 100 s

The eigen frequencies ω_+, ω_z, and ω_- can be measured independently. A high resolution Fourier transform of the induced voltage at ω_+ as shown in Fig. 6 demonstrates that the fractional statistical uncertainty of the center frequency

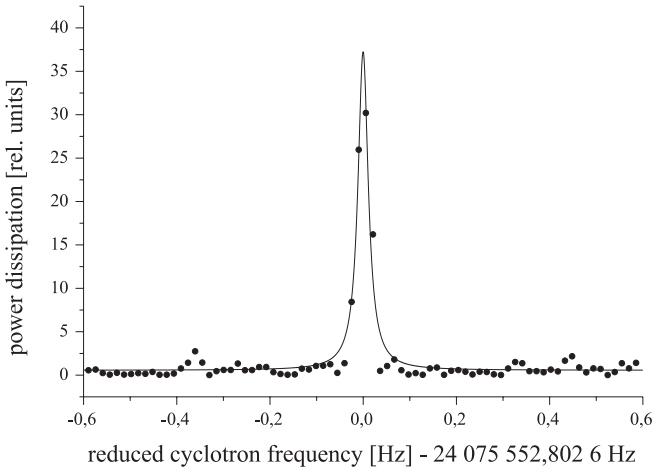

Fig. 6. Cyclotron signal of a single $^{12}C^{5+}$ ion. The full width of the resonance is 20 mHz corresponding to a relative line width of 10^{-9}. The measurement time is given by the Fourier limit to 80 s

is below 10^{-9}. ω_z and ω_- can also be measured sufficiently precise.

In order to measure the Larmor frequency ω_L we have to induce spin flip transitions by a microwave field at about 105 GHz and detect the spin direction. The detection is performed by a method introduced by Dehmelt for his $g-2$ experiment on the free electron [18] and called the "continuous Stern-Gerlach effect": A weak inhomogeneous magnetic field is superimposed to the homogeneous strong field at the center of one of the potential minima. It is created by the ferromagnetic nickel ring electrode of the analysis trap. The magnetic field strength near the center of the ring electrode now can be written as

$$B = B_0 + B_2 z^2 \, . \tag{7}$$

The total potential of a stored ion is the sum of the electric and magnetic potential $q\Phi$ and μB, respectively. Both Φ, the quadrupole potential, and the magnetic field B depend on the square of the axial coordinate. Thus the axial oscillation remains harmonic. The frequency, however, depends on the sign of μ, determined by the direction of the spin. We have designed the nickel ring electrode in such a way that the difference in the axial frequency for both spin directions is 0.7 Hz in a total frequency of 364 kHz [9]. Fig. 7 shows an example of the slight difference

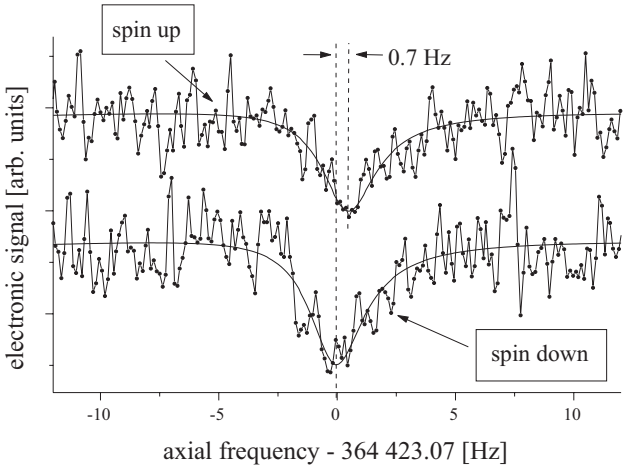

Fig. 7. Axial signal for two different spin directions of a single $^{12}C^{5+}$ ion. The averaging time was 1 min

in the axial oscillation frequency for the two spin directions. The averaging time here was 1 min. A continuous measurement of the spin direction via the axial oscillation frequency is shown in Fig. 8. The example is taken with high amplitude of the microwave field and its frequency close to the Larmor resonance.

4 Results

In order to obtain a Larmor resonance line we have to vary the frequency of the microwave field and count the number of spin flips per unit time. In order to avoid saturation effects the microwave field amplitude was kept low. The resonance curve obtained in the described manner is rather asymmetric. The lineshape can be described using the known spatial configuration of the magnetic field and a thermal distribution of the axial energy. A least squares fit to the data points as shown in Fig. 9 leads to a fractional uncertainty of about 10^{-6} and the g factor can be quoted with the same error [9].

A substantial improvement was obtained when we separated spatially the detection of the spin direction from the place where spin flips are induced. This was achieved by a transfer of the ion from the analysis trap to the precision trap. The potential minimum in which the ion was kept is moved by adiabatic change of the storage voltages at the trap electrodes. While in the analysis trap

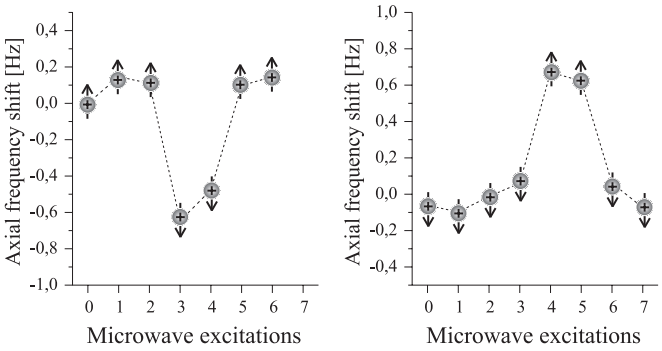

Fig. 8. Induced quantum jumps between the two spin directions of the electron bound in $^{12}C^{5+}$. At each measurement point first the ion is irradiated by microwaves and then the axial frequency of the ion is measured

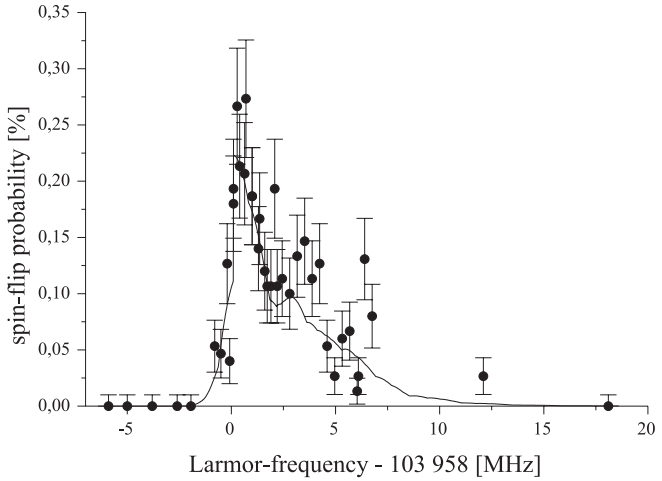

Fig. 9. This Larmor spectrum was measured in the analysis trap by resonant excitation (at 104 GHz) of the transition between the two spin states (spin up and down) of the bound electron. The asymmetric line shape of the resonance curve is due to the strong magnetic inhomogeneity in the analysis trap in combination with the thermal Boltzmann distribution of the ion's axial oscillation amplitude

the magnetic field is inhomogeneous as required for analysis of the spin direction the field is homogeneous in the precision trap and the Larmor and cyclotron frequency are defined very precisely. Since the axial oscillation frequency may not be exactly the same after an ion transfer back and forth an additional spin flip was induced in the analysis trap to make sure what the spin direction was before and after the transfer. As a consequence of this spatial separation the resonance line became much narrower and more symmetric.

A second improvement was that we measured the cyclotron frequency in the precision trap simultaneously with the Larmor frequency. This reduces to a large extent possible errors induced by a temporal variation of the magnetic field which occurs in superconducting solenoids typically at a level of 10^{-8} per hour. In the final experiment we measure the rate of spin flips at different ratios of the Larmor- and cyclotron field frequencies. An example is shown in Fig. 10. The linewidth is of the order of 10^{-8} and the g factor can be determined with a statistical uncertainty below 1 ppb [19].

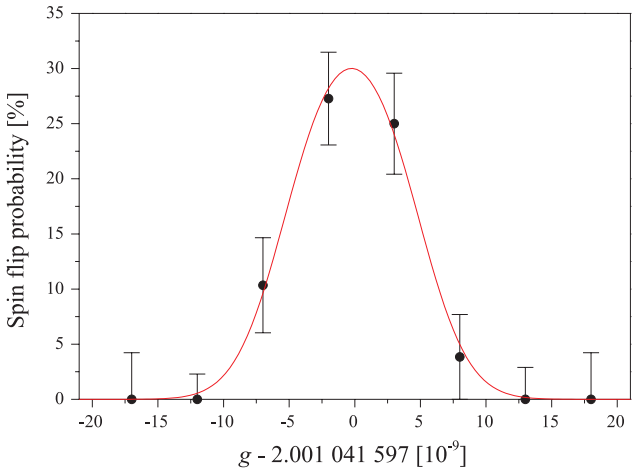

Fig. 10. Example of a Larmor resonance in the precision trap. Here the spin flip probability is plotted versus the ratio $g = 2\omega'_L/\omega_c^e$ of the microwave excitation frequency ω'_L and the electron's free space cyclotron frequency ω_c^e. This is convenient because this ratio is independent of the magnetic field

We have to account for a number of possible systematic shifts of the resonance. The largest arises from the fact that the cyclotron energy has to be of the order of a few eV to obtain a sufficiently strong signal from the induced voltage in the ring electrode. Since we have a small residual magnetic field inhomogene-

Table 2. Systematic errors of the g_J determination which are considered. All uncertainties are given in relative units

asymmetry of resonance	2×10^{-10}
measurement of cyclotron energy	2×10^{-11}
electric field imperfections	1×10^{-10}
magnetron energy	1×10^{-11}
relativistic corrections	1×10^{-12}
shift by standing microwave field	$< 10^{-14}$
stability of quartz oscillators	1×10^{-10}
grounding of apparatus	4×10^{-11}
interaction with image charges	3×10^{-11}
saturation of spin-flip transition	5×10^{-12}
spectral purity of microwaves	5×10^{-13}
cavity QED shifts	$\approx 10^{-13}$
damping of ion motion	$\approx 10^{-20}$
total (quadrature sum)	3×10^{-10}

ity even in the precision trap a finite cyclotron energy leads to a shift in the frequency. To account for that shift we have measured the g factor at different excitation amplitudes and extrapolated to zero energy. Remaining shifts such as electric field imperfections or relativistic shifts are small. The inhomogeneity of the magnetic field also leads to a slight asymmetry of the line because of thermal fluctuations in the axial energy. This is taken into account by a line shape formula which is a convolution of a Gaussian and a Boltzmann distribution. The difference in g factors between a symmetric and an asymmetric line shape fit is taken as the uncertainty. Table 2 gives an account of the uncertainties taken into consideration.

Our final result for the g factor of the electron bound in C^{5+} is [19]

$$g = 2.001\,041\,596\,4\ (8)\ (6)\ (44)\,. \tag{8}$$

The quoted error bars arise from statistical and systematical uncertainties and the uncertainty of the ratio ω_c^e/ω_c^i of the cyclotron frequencies of the electron and the $^{12}C^{5+}$-ion (electron mass), respectively.

The experimental value is in agreement with the present result of the theoretical calculation as quoted in section 2. It confirms the QED calculations of the order α/π on the 1 % level. It is also sensitive to the nuclear recoil correction.

5 Future Prospects

It seems likely that improvements on the experimental as well as on the theoretical side will happen in the near future. Experimentally the width of the g factor resonance as shown in Fig. 10 can be explained by the residual inhomogeneity of the magnetic field in the precision trap where spin flips take place. It is caused

by the nickel ring electrode in the analysis trap at a distance of 2 cm. A new trap with larger distance between the two traps will reduce this limitation in linewidth. At the same time additional shimming coils in the superconducting solenoid may be used to eliminate further the field inhomogeneity at the precision trap. The effect of these improvements would be a narrower linewidth as well as a reduction of the influence of the finite cyclotron energy on the g value which at present represents the largest part of the systematic error. We expect an overall improvement by about one order of magnitude.

It should be noted that the technique of g factor measurements described above is applicable to any Hydrogen-like ion with zero nuclear spin provided the ion can be produced and injected into the trap. The Larmor frequency varies for all those ions throughout the periodic systems by at most 15 % (Fig. 1). The axial oscillation frequency depends on $\sqrt{q/m}$ which is of the same order of magnitude for all Hydrogen-like ions. The fractional change in axial frequency upon a spin flip, however, scales inversely to the mass of the ion. Thus a stronger inhomogeneity of the magnetic bottle field is required for spin flip detection, when working with high Z-ions. This may represent a technical difficulty. It can, however, partially be compensated by longer averaging times.

On the theoretical side improvements are likely as well. Although the bound state QED calculations are much more difficult than those for the free electron and a complete evaluation of all contributions to the order $(\alpha/\pi)^2$ is rather tedious it may be possible to evaluate at least some of the leading terms of that order in the near future [13,14,15]. This would reduce the uncertainty in the estimate of the remaining contributions. It may even not be necessary to evaluate the complete higher order contribution. As pointed out by S. Karshenboim the general structure of these terms may be known without explicit knowledge of the corresponding numerical value of the $(\alpha/\pi)^2$ coefficient [15]. Measurements of the g factors of different low-Z Hydrogen-like ions allows to determine this coefficient experimentally.

Anticipating improvements on the experimental and theoretical side a number of interesting possibilities for future experiments arise:

5.1 Electron Mass

As seen from Eq. 8 the uncertainty of the electron mass in atomic units is the largest part of the total experimental uncertainty. If we take the theoretical value for the g factor in C^{5+} (Eq. 3) for granted we can determine a value of the electron mass from our experimental g factor:

$$m_e = 0.000\,548\,579\,912\,8\ (3)\ (15)\ \text{u}\ . \tag{9}$$

The first error comes from the experimental uncertainty of our g factor measurement and the second represents the uncertainty of the theoretical calculations. Our value is in agreement with that determined directly by comparison of the electrons cyclotron frequency to that of a ^{12}C nucleus in a Penning trap by van Dyck and coworkers [16]. It gives

$$m_e = 0.000\,548\,579\,911\,1\ (12)\ \text{u} \tag{10}$$

It is evident that any improvement in the theoretical calculation will lead to a new and more precise value of the electron mas. This is particularly the case when working with low-Z ions such as He^{+}, Li^{2+}, Be^{3+} [15], since the uncalculated higher order QED terms have here only a small influence on the g factor and the uncertainty of the lower order calculation is small.

5.2 Fine Structure Constant

Once the electrons mass is known to a better accuracy it may be possible to derive a new value for the fine structure constant α from g factor measurements. The leading bound state correction to the g factor is the Breit term (Eq. 2). From that we deduce

$$\frac{\delta\alpha}{\alpha} = \frac{1}{(Z\alpha)^2}\frac{\delta g}{g} \,. \tag{11}$$

Thus for a determination of α from a g factor measurement it would be desirable to choose an ion where Z is sufficiently high to get a small uncertainty in α but the influence of higher order QED contributions is not too large. Ca^{19+} seems to be a good choice. If we assume the same experimental accuracy on that ion as presently obtained in C^{5+} we would obtain a fractional uncertainty in α of $8 \cdot 10^{-8}$. This is comparable to other present determinations of α from Quantum Hall or Josephson effect. The envisaged improvement in the experimental g factor by one order of magnitude would make the α determination competitive with that extracted from the g factor of the free electron.

5.3 Electron Binding Energies

As seen from Fig. 6 the cyclotron frequency of a stored ion in the precision trap has a full width of about 10^{-9}. The center frequency can be conservately determined to 10^{-10}. Provided the magnetic field is stable in time at the same level, the cyclotron frequencies and consequently the masses of different charge states can be compared very precisely.

The mass M_i of an ion in a charge state i is composed of the mass of the bare nucleus M_{nuc}, the mass of the electrons $(Z-i)\,m_e$ and the negative binding energy E_{B}. Two ions of charge state i and $i-1$ differ by the binding energy E_{B}^{i} of the outermost electron and its mass. Thus from a comparison of the corresponding two cyclotron frequencies we can determine E_{B}^{i}:

$$\frac{\omega_{c,i}}{\omega_{c,i-1}} = \frac{q_i}{q_{i-1}}\frac{M_i c^2 - m_e c^2 - E_{\mathrm{B}}^{i}}{M_i c^2} \,. \tag{12}$$

A precision of the order of 10^{-10} in the cyclotron frequency corresponds to a mass uncertainty of about 1 eV for low-Z ions and 10 – 20 eV for high Z. The binding energies range from a few eV to several keV. They can be calculated including correlation energies between the electrons due to their Coulomb interaction and their magnetic interaction (Breit interaction) and radiative QED effects (self-energy and vacuum polarization)[20]. The differences in the values of E_{B}^{i} using

different theoretical approaches are typically of the order of 10 – 20 eV [20]. For light elements such as Carbon the experimental uncertainty will be well below that number while for higher Z values one would expect the same order of magnitude in the uncertainty. In any case the comparison of cyclotron frequencies of different charge states of an element provides a very good tool to test atomic binding energy calculations.

5.4 Nuclear Magnetic Moments

When using odd isotopes of an element having non-zero nuclear spin we have to take the hyperfine interaction into account. In the presence of a magnetic field the corresponding energy levels for Hydrogen-like ions are shifted according to the Breit-Rabi formula [21]. From transition frequencies between different m_F Zeeman substates one can derive electronic as well as nuclear g factors. While induced electronic spin transitions can be detected in the manner described above for even isotopes, a nuclear spin transition can be observed in a double resonance experiment: The transition rate for an electronic spin flip, induced between $F = 1, m_F = 0$ and $F = 1, m_F = -1$ changes, when a radiofrequency transition between the $F = 1, m_F = 0$ and $F = 1, m_F = +1$, corresponding to a nuclear spin flip, is driven (Fig. 11). A practical requirement for such a

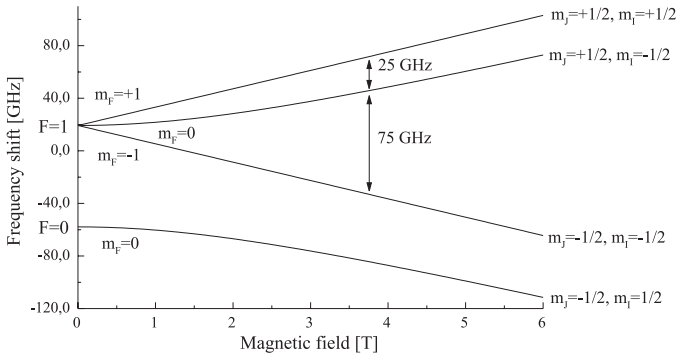

Fig. 11. Breit-Rabi diagram for $^{13}C^{5+}$

measurement is that the lifetime of the hyperfine structure levels is at least a few minutes. This is the case only for low-Z ions approximately up to $Z = 20$. For higher Z we would have to measure the g_F value of the lower hyperfine level and extract the g_I factor with the corresponding g_J factor taken from an even isotope as an additional input to the Breit-Rabi formula.

The knowledge of nuclear moments from Hydrogen-like ions would allow to determine experimentally the shielding of the outer magnetic field by the elec-

tron cloud in a multi-electron system (diamagnetic correction). This correction is typically of the order of $10^{-4} - 10^{-5}$ but can for heavy atoms be as large as 10^{-2} [22]. So far the diamagnetic correction has to be calculated since no measurement on bare nuclei or Hydrogen-like systems are available for comparison. Measurements on Hydrogen-like ions may also contribute to the solution of a problem appearing in recent hyperfine structure measurements on Hydrogen-like U^{91+} and Pb^{81+}: The measured ground state hyperfine separation disagrees with theoretical calculations, possibly because of incorrect values of the nuclear magnetic moments, which are taken from NMR measurements [22,23].

Also it would be possible to determine experimentally the influence of the electron shell to the nuclear wave function (nuclear polarizability). The 1S-electrons in heavy atoms admix excited states to the ground state of the nucleus in the order of 10^{-3} [24]. This leads additionally to the diamagnetic shielding to observable differences in the order of 10^{-3} of the nuclear magnetic moments for different charge states.

5.5 Lithium-like Ions

Advances in high precision variational techniques allow to determine essentially exact solutions of relativistic energy eigenvalues for few-electron systems. Radiative corrections can also be taken into account. This has led to good agreement between experimental and theoretical values of Lamb shifts in Lithium-like systems where QED contributions are tested at the 0.2% level [25]. No corresponding calculations for the g factor of the unpaired electron exist so far to our knowledge. Measurements on Lithium-like ions at a similar level of accuracy as in Hydrogen-like ions are possible using the present setup in our laboratory and might stimulate calculations testing our understanding of correlation effects between the electrons.

Acknowledgements

We acknowledge stimulating discussions with S. Karshenboim, Th. Beier, I. Lindgreen, A. Yelkhowski, V. Shabaev, K. Pachucki, and with V. Natarajan. Our work was financially supported by the European Union under the contract number ERB FMRX CT 97-0144 within the Eurotraps network.

References

1. R.S. Van Dyck, Jr., P.B. Schwinberg and H.G. Dehmelt: Phys. Rev. Lett **59**, 26 (1987)
2. V.W. Hughes and T. Kinoshita: Rev. Mod. Phys. **71**, 133 (1999)
3. For a review see: V.M. Shabaev: in "Atomic Physics with Heavy Ions" (F. Beier and V.P. Shevelko, eds.) Springer 1999, pp. 139–159
4. H. Persson, S. Salomonson, P. Sunnergreen and I. Lindgreen: Phys. Rev. A **56**, R2499 (1997)
5. J. S. Tiedeman and H. G. Robinson: Phys. Rev. Lett. **39**, 602 (1977).

6. C. E. Johnson and H. G. Robinson: Phys. Rev. Lett. **45**, 250 (1980).
7. P. Seelig *et al.*: Phys. Rev. Lett. **81**, 4824 (1998)
8. V.M. Shabaev: Can. J. Phys. **76**, 907 (1998).
9. N. Hermanspahn *et al.*: Phys. Rev. Lett. **84**, 427 (2000)
10. G. Breit: Nature **122**, 649 (1928)
11. A. Blundell, K.T. Cheng and J. Sapirstein: Phys. Rev. A **55**, 1857 (1997)
12. Th. Beier *et al.*: Phys. Rev. A **62**, 032510 (2000)
13. Th. Beier, I. Lindgreen, H. Persson, S. Salomonson, P. Sunnergreen *this edition*, pp. 605–618
14. S. Karshenboim, K. Pachucki, A. Yelkhowsky, Th. Beier: private communication
15. S. Karshenboim *this edition*, pp. 651–663
16. R.S. Van Dyck Jr., D.L. Farnham and P.B. Schwinberg: Physica Scripta **T59**, 134 (1995)
17. D.J. Wineland and H.G. Dehmelt: Journal of Appl. Phys. **46**, 919 (1975)
18. H. Dehmelt: Proc. Natl. Acad. Sci. USA **53**, 2291 (1986)
19. H. Häffner *et al.*: Phys. Rev. Lett. (submitted)
20. J. Sapirstein: in "Trapped Charged Particles and Fundamental Physics", Asilomar, Calif. 1998 (D. Dubin and D. Schneider eds.). AIP Conference Proceedings **457**, pp. 3–12 (1999)
21. N.F. Ramsey: Molecular Beams, Oxford (1956)
22. M.G.H. Gustavsson and A.-M. Martensson-Pendrill: Phys. Rev. A **58**, 3611 (1998)
23. V.M. Shabaev, A.N. Artemyev and V.A. Yerokhin: AIP Conference Proc. **457**, 22 (1999)
24. B. Hoffmann, G. Baur, J. Speth: Z. Phys. A **315**, 57 (1984)
25. V.M. Shabaev, A.N.Artemyev and V.A.Yerokin: Physica Scripta **T86**, 7 (2000)